

Supplementary Information

to

pH-dependent structural alterations in LHCII revealed by two-dimensional infrared spectroscopy

Thanh Nhut Do, Kinga Hajduk, Roberta Croce, and John T.M. Kennis*

Department of Physics and Astronomy, Faculty of Science, Vrije Universiteit Amsterdam, De Boelelaan 1100, 1081 HZ Amsterdam, The Netherlands.

*Corresponding author: j.t.m.kennis@vu.nl

Contents

S1 Steady-state fluorescence spectra	2
S2 Quasi-TA spectra extracted from two 2DIR spectra	2
S3 Cross-peak centers determination	3
S4 Experimental procedures	4
References	8

S1 Steady-state fluorescence spectra

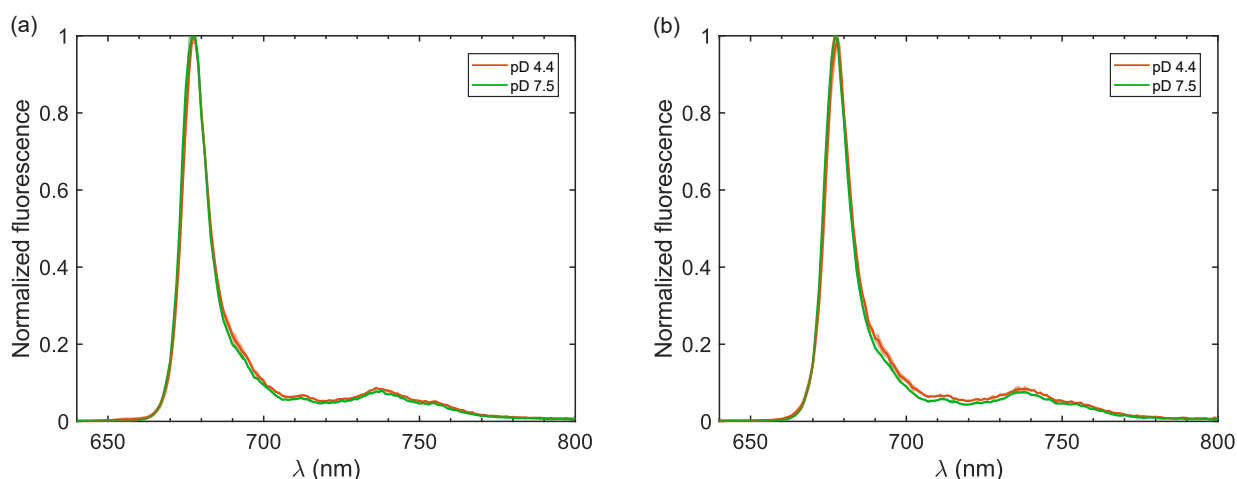


Figure S1. 77-K steady-state fluorescence spectra of LHCII at two pD conditions, excited at 475 nm (a) and 500 nm (b).

Low temperature (77 K) steady-state fluorescence spectra of LHCII measured with two different excitation wavelengths are presented in Figure S1. The excitation wavelength of 475 nm and 500 nm were used to preferentially excite Chls b and carotenoids, and the resultant spectra are virtually identical. The lack of F700 band indicates that there was no aggregation induced in our samples. The almost identical steady-state fluorescence spectra among all three excitation wavelengths further indicate that the fluorescing states of LHCII trimers in our experimental conditions are identical regardless what pigments were excited.

S2 Quasi-TA spectra extracted from two 2DIR spectra

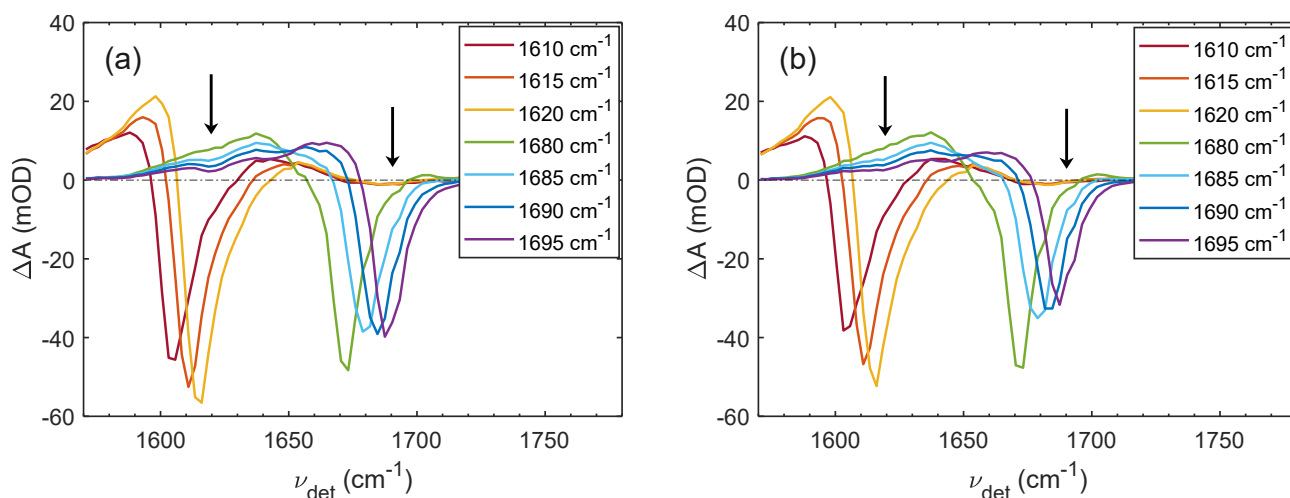


Figure S2. Quasi-transient absorption (quasi-TA) spectra extracted by taking horizontal slices from 2DIR spectra of Figure 4(a-b) of the main text at the denoted excitation frequency ν_{exc} in the legend. The arrows indicate the position of β coupling cross-peaks discussed below.

The quasi-TA spectra extracted at low-frequency region $\nu_{exc} = 1610\text{-}1620\text{ cm}^{-1}$ and the high-frequency region $\nu_{exc} = 1680\text{-}1690\text{ cm}^{-1}$ are plotted in Figure S2(a, b) without any intensity rescaling to give an impression on how small the β -cross-peaks are compared to the major α -helices' signal. Once again, comparing Figures S2(a) and (b), we barely notice any difference. The low-frequency quasi-TA spectra ($\nu_{exc} = 1610\text{-}1620\text{ cm}^{-1}$) in both pDs exhibit a very strong GSB diagonal signal, accompanied by a corresponding positive red-shifted ESA signal. The high-frequency ends of these quasi-TA spectra all go up, change sign to the positive, and all three of them drop back to the same negative maximum at around $\nu_{det} = 1690\text{ cm}^{-1}$.

Oppositely, the high-frequency quasi-TA spectra ($\nu_{exc} = 1680\text{-}1695\text{ cm}^{-1}$) show a negative diagonal GSB peak with the corresponding positive ESA band, which extends towards the lower-frequency region. Except for the 1680-cm^{-1} quasi-TA spectrum, the rest of them exhibit a small but noticeable negative peak at the same frequency at around $\nu_{det} = 1620\text{ cm}^{-1}$. In this case, the cross-peaks are somewhat clearer in the pD-4.4 spectra [Figure S2(a)] compared to the pD-7.5 ones [Figure S2(b)]. Hence, the quasi-TA spectra extracted from the Δ 2DIR spectrum were inspected and discussed in the main text.

S3 Cross-peak centers determination

As reported previously, the two excitonically coupled vibrational modes specifically formed with β -motifs can be used to estimate the extension degree of the β -sheets, i.e., how large the β -sheet is. The high-frequency mode ν_{\parallel} is less sensitive to the β -sheet size and roughly centers at 1690 cm^{-1} .¹ Hence, we will focus on the low-frequency mode ν_{\perp} , which exhibit stronger dependence on the β -sheet size.¹

Quasi-TA spectra extracted at $\nu_{exc} = 1690$ and 1695 cm^{-1} were subjected to Gaussian decomposition, focusing on the cross-peak region of $\nu_{det} = 1580\text{-}1630\text{ cm}^{-1}$. In total, six quasi-TA spectra were subjected to the fit [two ν_{exc} times three 2D spectra (two 2DIR spectra of pD 4.4 and 7.5 and the Δ 2DIR spectrum)]. Each quasi-TA spectrum was fit with three Gaussian peaks. Two of them have positive amplitudes, representing two ESA signals of the cross-peak (centered around $1605\text{-}1610\text{ cm}^{-1}$) and the large diagonal peak (centered around 1640 cm^{-1}), which is not included in the region of interest. One Gaussian peak having a negative amplitude is the GSB signal of the cross-peak showing the frequency of the ν_{\perp} mode.

Figure S3 clearly shows that the negative Gaussian peak always stay at the same frequency of around $1622 \pm 4\text{ cm}^{-1}$ in both pDs and the Δ 2DIR difference spectrum as well. Hence, we can conclude that the sizes of the β -sheets observed in both pDs were the same within the fit uncertainty, only the amount of β -sheets increases upon acidification. We note that in Figures S3(a,b,d,e), the red-shifted ESA peak centered around 1610 cm^{-1} is strongly influenced by the large ESA signal of the diagonal features (not in range), represented by a large Gaussian at 1640 cm^{-1} . Hence, we do not further analyze the cross-peak's ESA signals.

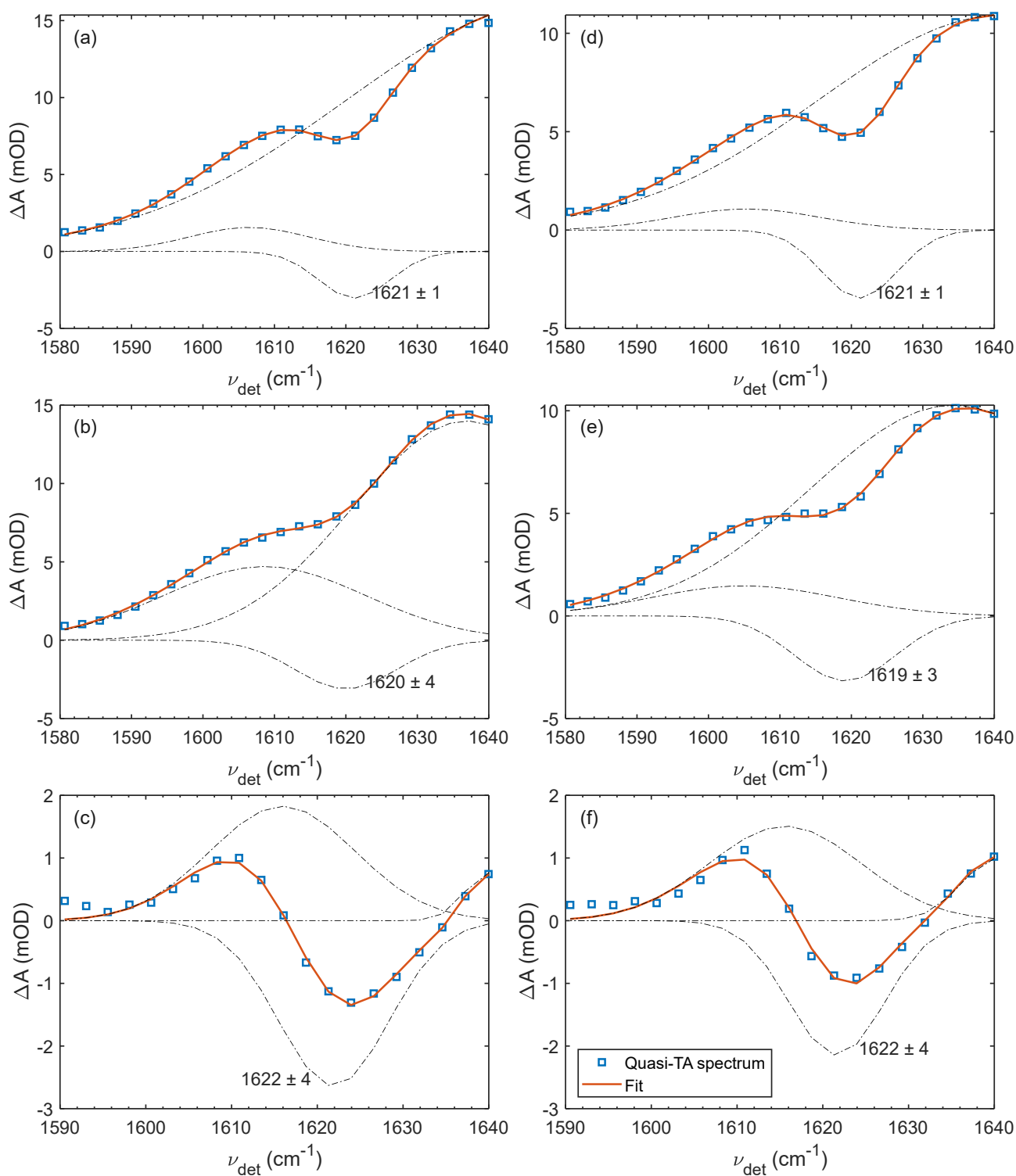


Figure S3. Gaussian decomposition results of six quasi-TA spectra extracted at $\nu_{exc} = 1690 \text{ cm}^{-1}$ (a-c) and 1695 cm^{-1} (d-f). Each row are two quasi-TA spectra obtained as horizontal slices from the 2DIR spectrum at pD 4.4 (a, d), pD 7.5 (b, e) and the Δ 2DIR spectrum (c, f). The black dash-dotted lines depict three Gaussian peaks obtained for each fit. The fitted value of the negative Gaussian peak center is added to each panel with the 95% confidence interval.

S4 Experimental procedures

Growth conditions of *Arabidopsis thaliana* and preparation of LHCII

A. thaliana WT (Col-0) plants were grown for five weeks under a 12h/12h day/night

photoperiod and a photon flux of $120 \mu\text{mol m}^{-2}\text{s}^{-1}$. Prior to thylakoid isolation, plants were dark-adapted for at least 2 hours. Thylakoid membranes were prepared according to Xu *et al.*'s protocol.² For sucrose gradient ultracentrifugation, membranes were solubilized following the method of Caffari *et al.*,³ with modifications as detailed below.

Thylakoids were unstacked in 5 mM EDTA and subsequently washed with 10 mM HEPES pH 7.5. Membranes were solubilized at a final chlorophyll concentration of 1 mg/mL using an equal volume of 1.2% (w/v) α -DDM for 10 minutes. Insoluble material was removed by centrifugation at $15000\times g$ for 10 minutes, and the supernatant was applied onto 0.1-1 M sucrose gradient containing 0.06% α -DDM and 10 mM HEPES pH 7.5. For samples prepared at pH 4.4, all the buffers were replaced with citrate buffer and adjusted to pH 4.4.

The gradients were centrifuged at 40000 RPM for 17 h at 4 °C using SW41 rotor (Beckman-Coulter). The LHCII trimer band was collected and subjected to buffer exchange using Amicon Ultracentrifugal filters, 10 kDa MWCO (Millipore). Samples were concentrated to approximate one-tenth of their volume, diluted with the corresponding D₂O-based buffer and reconcentrated. This exchange step was repeated three times.

Absorption and CD

Both visible absorption and CD spectra of all samples were measured using Chirascan plus instrument (Applied Photophysics). A small amount ($\sim 0.1 \mu\text{L}$) of the concentrated sample after deuterated buffer exchange was diluted with the corresponding buffer until the Q_y absorption maximum reached ~ 0.6 - 0.8 OD/cm. The baseline of each absorption and CD measurement was recorded right before each measurement using the corresponding buffer in a 1-cm pathlength quartz cuvette. The baselines were subtracted from the presented spectra.

Steady-state fluorescence

Fluorescence emission spectra were recorded at 77 K using a Fluorolog 3.22 spectrofluorometer (Jobin-Yvon-Spex) equipped with a cold finger. All measurements were performed on samples adjusted to an optical density of below 0.03 OD/cm at the Q_y absorption maximum.

Time-correlated single photon counting

Fluorescence decay kinetics were measured using a FluoTime200 fluorometer (PicoQuant). Samples were excited with a 440-nm laser diode ($5 \mu\text{W}$) operating at a repetition rate of 10 MHz, and fluorescence emission was detected at 680 nm. All measurements were performed on samples diluted to an optical density of less than 0.05 OD/cm at the Q_y absorption maximum. Samples were maintained at 10 °C and continuously stirred in a 1-cm cuvette during data acquisition. The IRF approx. 92 ps full-width at half-maximum was determined using the pinacyanol iodide dye dissolved in methanol, as described previously.⁴

Fourier transform infrared spectroscopy

The samples used for FTIR and 2DIR measurements were concentrated until the optical density of the Amide I band reached ~ 0.5 OD for 50- μm pathlength. All FTIR spectra were

recorded using the IFS 66/S instrument (Bruker). A globar was used as mid-IR light source covering the frequency range of 500-6000 cm^{-1} . After being split into two interferometric arms by a KBr beamsplitter and guided by a HeNe continuous laser, the IR light was focused on the sample mounted in an enclosed sample chamber with continuous purging by compressed N_2 gas to minimize the interference from water vapour's absorption lines. The sample droplet was held between two CaF_2 windows with a 50- μm Teflon spacer. Around 10-15 μL volume of sample was used for each measurement to ensure a complete filling of the window surface, avoiding air bubbles which can cause etalon interference. The transmitted IR light was then focused on a single-element mercury-cadmium-telluride (MCT) detector (Kolmar Technologies) cooled with liquid nitrogen. The interferograms were recorded with 20-kHz scanning speed, double zero-padded and phased before Fourier transformed to yield the FTIR spectra. Each FTIR spectrum was averaged with 20-50 acquisitions. The same optics were used to assemble the buffer and protein samples to minimize any systematic baseline. FTIR spectra of both deuterated buffer and protein sample were recorded consecutively for every measurement to maximize the confidence of baseline subtraction procedure.

Two-dimensional infrared spectroscopy

2DIR measurement was implemented using the pulseshaper-assisted partially collinear pump-probe geometry. The 800-nm 1-kHz 35-fs output from a regenerative amplifier (Spitfire, SpectraPhysics) was sent to a dual stage optical parametric amplifier (TOPAS-C, Light Conversion) to generate two near-IR outputs of 1400 nm and 1800 nm. Two near-IR beams were then split by a dichroic mirror and the 1800-nm beam was reflected on a motorized delay stage to control the inter-pulse delay time. After being recombined on the second dichroic mirror, two near-IR beams were mixed on a AgGaS_2 crystal to generate the difference-frequency signal having duration of around 200 fs and centered around 6 μm , corresponding to the maximum of the Amide I frequency of 1650 cm^{-1} . The mid-IR beam was then sent to an enclosed, dried-air purged optical setup and split into two paths. The pump path was sent through the acousto-optic modulator (AOM) 4-f pulseshaper (Quichshape, PhaseTech), where the pump pulses were shaped by acoustic waveforms generated computationally and loaded into a germanium AOM placed in the Fourier-plane of the pulseshaper.⁵ The pump pulses were shaped into double-pulse trains with inter-pulse delay time τ scanned from 0 to 3800 fs with 40-fs steps. The partial rotating frame frequency was set to 1450 cm^{-1} to reduce the coherent oscillation frequency, allowing undersampling with 40-fs τ -steps. The phase of individual pulse in each double-pulse train was cycled between 0 and π , yielding 4 phase combinations for each waveform, which were then combine to reconstruct the coherence interferogram, i.e., τ -dependent TA spectra, with minimized scattering signal.⁶ The probe beam was reflected by a gold-coated corner cube, mounted on a motorized delay stage, to control the population time. In this study, the pump-probe delay time, i.e., population time, was kept at 500 fs. The polarization of the pump was set to be perpendicular with respect to the probe's one (ZZYY polarization scheme) by a mid-IR $\lambda/4$ waveplate, placed at the output port of the pulseshaper. Both pump and probe beams were then focused on the sample mounted

similarly as in the FTIR measurements. A wire grid polarizer (Thorlabs) was placed right after the sample to cut-off the residual pump lights in order to avoid any interference on the detector. The transmitted probe beam was then routed to a spectrograph (Chromex) and detected by a dual row 64-element MCT array (InfraRed Associates, Inc.) cooled with liquid N₂. To minimize any systematic error and ensure the same laser conditions, the 2DIR spectra of two LHCII samples were always measured subsequently on the same day and the Δ 2DIR spectra was always calculated with the two 2DIR spectra of the same pair.

References

- (1) Lomont, J. P.; Ostrander, J. S.; Ho, J.-J.; Petti, M. K.; Zanni, M. T. *The Journal of Physical Chemistry B* **2017**, *121*, 8935–8945.
- (2) Xu, P.; Tian, L.; Kloz, M.; Croce, R. *Scientific Reports* **2015**, *5*, 13679.
- (3) Caffarri, S.; Croce, R.; Breton, J.; Bassi, R. *Journal of Biological Chemistry* **2001**, *276*, 35924–35933.
- (4) Van Oort, B.; Amunts, A.; Borst, J. W.; van Hoek, A.; Nelson, N.; van Amerongen, H.; Croce, R. *Biophysical Journal* **2008**, *95*, 5851–5861.
- (5) Ghosh, A.; Serrano, A. L.; Oudenhoven, T. A.; Ostrander, J. S.; Eklund, E. C.; Blair, A. F.; Zanni, M. T. *Optics Letters* **2016**, *41*, 524.
- (6) Hamm, P.; Zanni, M., *Concepts and Methods of 2D Infrared Spectroscopy*; Cambridge University Press: 2011.